J. Membrane Biol. 140, 69–79 (1994)

The Journal of
Membrane
Biology

Modulation of Small Conductance Calcium-activated Potassium Channels in C6 Glioma Cells

D. Manor, N. Moran
Department of Neurobiology, The Weizmann Institute, Rehovot 76100, Israel

Received: 16 November 1993/Revised: 9 February 1994

Abstract. Using the patch clamp technique, we have characterized a small conductance, calcium-activated potassium (SK) channel in the C6 glioma cell line. Elevation of cytosolic Ca^{2+} concentration ($[Ca^{2+}]_i$) by applications of serotonin or ionomycin induced bursts of channel openings recorded in the cell-attached configuration. These channels underlie the serotonin-induced, $[Ca^{2+}]_i$-activated whole-cell K^+ conductance described previously. $[Ca^{2+}]_i$ directly activated SK channels in inside-out patches with a biphasic concentration dependence. Submicromolar $[Ca^{2+}]_i$ induced bursts of channel openings with a unitary conductance of about 25 pS, similar to that of the serotonin-induced channels. Supramicromolar $[Ca^{2+}]_i$ caused prolonged openings with a unitary conductance of about 35 pS, resulting in a pronounced increase of the average current in patches exposed to $[Ca^{2+}]_i$ above 100 μM. The two modes of opening reflect the activity of the same SK channel. The channel conductance depended on external K^+ concentration with K_D of 5 mM. The channel was slightly permeable to cations other than K^+, with a permeability ratio for K^+:Ca^{2+}:Na^+ of 1:0.040:0.030, respectively. ATP was required to maintain channel activity in outside-out patches but was not essential in inside-out patches. The modulation of SK channels in C6 cells by components in their microenvironment may be related to the role of glial cells in controlling the extracellular milieu in the CNS.

Key words: SK channels — ATP — Serotonin — Sublevels — Patch clamp — Glia

Correspondence to: D. Manor

Introduction

Elevation of cytosolic free Ca^{2+} concentration ($[Ca^{2+}]_i$) induces activation of K^+ channels in many cell types [3, 6, 9, 10, 29, 36]. These channels, defined by their high selectivity for potassium ions, are divided roughly in two classes [5, 19, 22]. The BK (big K^+) channels have large conductance in the 100–200 pS range, the efficacy of their activation by cytosolic Ca^{2+} increases with membrane depolarization, and they are sensitive to TEA in the mM concentration range and to charybdotoxin in the nM range. The SK (small K^+) channels have lower conductance (mostly under 50 pS); they are activated by submicromolar $[Ca^{2+}]_i$ independently of membrane potential (V_m), and are usually blocked by apamin but not by TEA in the millimolar range [4, 27].

Relative to the wealth of information already existing on other K^+ channels [1, 15, 16], the information concerning the SK channels has been rather limited. The voltage independence of SK channel activation [4, 7] may be of special significance in nonexcitable cells that do not readily depolarize under physiological conditions, but do respond to stimuli with a rise in $[Ca^{2+}]_i$, mobilized from intracellular stores. The C6 glioma cell line serves as a convenient model for nonexcitable cells. We and others have shown already that the application of an appropriate transmitter onto these cells releases Ca^{2+} from inositol trisphosphate (IP_3)-sensitive intracellular stores leading to the activation of K^+ membrane conductance [21, 23, 26, 30]. Thus, the aim of the present study was to characterize the SK channels underlying the whole-cell potassium conductance evoked by the application of serotonin (5-hydroxytryptamine, 5-HT) in the C6 glioma cell line. The SK channels we found possess unique features, including dynamic response to a wide $[Ca^{2+}]_i$ range, a non-negligible permeability to Na^+ and Ca^{2+}, and an ATP requirement for sustained activity, depending on patch configuration.

Materials and Methods

C6 cells were cultured in DMEM supplemented with 10% heat-inactivated horse serum. They were plated on fire-cleaned 12 mm coverslips 24–48 hr before use.

Patch clamp experiments [11] were performed after placing a coverslip in a small volume perfusion chamber (150–200 μl). Thin-wall borosilicate glass pipettes (1.5 mm outer diameter) were pulled on a vertical puller, and fire-polished to yield a tip diameter of approximately 1 μm.

Tightly sealed membrane patches in the cell-attached, inside-out (I-O) or outside-out (O-O) configurations were voltage-clamped using an Axopatch-1B amplifier and a software-hardware control (pCLAMP program, TL1 and TM-100 Labmaster A/D and D/A peripherals; Axon Instruments, Foster City, CA). Current was filtered through a 0.5–1 kHz (−3 dB) cutoff frequency 4-pole Bessel filter, and was digitized and stored for further analysis on VCR cassettes (PCM Neurocorder from Neurodata).

The different external solutions were mixtures of the following stock solutions, all buffered to pH 7.4 (concentrations in mM): (1). KCl (or K-gluconate) 140, HEPES/KOH 10, $MgCl_2$ 2; (2). NaCl 140, HEPES/NaOH 10, $MgCl_2$ 2, $CaCl_2$ 2; (3). Ca-(gluconate)$_2$ 50, TRIS/gluconate 10, $MgCl_2$ 2, Mannitol 150; (4). $CaCl_2$ 100, Tris/HCl 5, $MgCl_2$ 2; (5). *N*-methylglucamine (NMG)/methane-sulfonate (MS) or NMG-chloride 140, HEPES/NMG 10, $MgCl_2$ 2. The solution at the intracellular surface of the patch contained (in mM): KCl 140, HEPES/KOH 10 (pH 7.4) and $MgCl_2$ 1. $CaCl_2$ in the internal solution was buffered with 1 mM of the Ca^{2+} buffer BAPTA (K_D = 110 nM) to yield the desired $[Ca^{2+}]_i$ in the submicromolar range. $CaCl_2$ without buffer was used to obtain $[Ca^{2+}]_i$ in the supramicromolar range. In the outside-out configuration 1 mM ATP was also added to the pipette solution. Activities, rather than concentrations, were used in Fig. 2*B*, 10 and 12, Eqs. (1) and (4) and in Table 2 (calculated using activity coefficients from Robinson and Stokes [28]). In all other cases, we referred to the nominal concentrations of the constituents of the solutions. Serotonin (1–100 μM) or ionomycin (1 μM) were pressure-ejected from a micropipette, with less than 1 μm tip, situated near the cell.

Experiments were conducted in room temperature, ranging between 22–26°C, with variation of less than 2°C during any particular experiment.

Data Analysis

Data were analyzed using the pCLAMP software, and commercially available programs for PC (Matlab, The MathWorks, Natick, MA) or Macintosh (KaleidaGraph). Pooled data are presented as mean ± SEM. To extract the relative permeability parameters P_{Ca} and P_{Na}, we rearranged Eq. (4) into a polynomial, derived the roots from the coefficient of the polynomial for each experimental value of $[Ca^{2+}]_i$, and minimized the difference between the observed reversal potential and that calculated from the positive solution of the polynomial (using Fortran NAG Library, National Algorithm group, UK). Notation: to avoid confusion, we used V_p and V_{rev} to denote pipette potentials in the "cell-attached" configuration, relative to the ground bath. Otherwise, E_M and E_{rev} are used to denote the (respective) potentials at the cytoplasmic side of the membrane relative to the ground.

Chemicals were purchased from Sigma (5-HT, ionomycin, ATP) and Calbiochem, Lucerne, Switzerland (BAPTA).

Abbreviations

5-HT:	5-hydroxytryptamine
ATP:	adenosine 5′-triphosphate
BAPTA:	1,2-bis(2-aminophenoxy)ethane-*N,N,N′,N′*-tetraacetic acid
HEPES:	4-(2-hydroxyethyl)piperazine-*N′*-(2-ethanesulfonic acid)
I-O:	inside-out
IP_3:	inositol 1,3,4-trisphosphate
NMG:	*N*-methyl-D-glucamine
O-O:	outside-out
TEA:	tetraethylammonium

Results

Spontaneous, Serotonin-induced and Ca^{2+}-activated K^+ Channels

In the cell-attached configuration, in most patches, we observed spontaneous activity of a few fast-gated channels (i.e., flickering in bursts, with an average open time, $\bar{t}_{open}$, of about 5 msec, Table 1). Short (3–12 sec) applications of 5-HT induced bursts of channel openings (Fig. 1) were recognizable above the background of spontaneous activity. Tiny fluctuations observed sporadically in the wake of the 5-HT-induced bursts (Fig. 1) have not been studied here. Occasionally, the amplitude of the channels during the 5-HT-induced activity increased transiently (*not shown*), reflecting membrane hyperpolarization of the whole cell. In other cases, the resting potential of the cell may have been already at E_K (the potassium reversal potential), perhaps due to the predominance of K^+ permeability of the cell membrane at rest, and therefore did not hyperpolarize

Table 1. Conductance and gating of SK channels in C6 cells in different recording configurations, in symmetrical 140 mM K^+ solutions (in excised patches and the cell-attached pipette)

Configuration	Trigger	γ(pS)[a]	$\bar{t}_{open}$(ms)[b]
On-Cell	5-HT	24 ± 3	4.4 ± 1.0
		n = 3	*n* = 3
	Ionomycin	23 ± 6	6.7 ± 1.1
		n = 2	*n* = 4
	Spontaneous	23 ± 1	4.7 ± 1.1
		n = 14	*n* = 6
I-O	$[Ca^{2+}]_i$	21 ± 2	1.4 ± 0.2
	600–900 nM	*n* = 12	*n* = 6
O-O	$[Ca^{2+}]_i$	26 ± 4	6.1 ± 0.7
	600–900 nM	*n* = 4	*n* = 6

[a] γ: Single channel conductance, mean ± SEM from *n* patches.
[b] $\bar{t}_{open}$: Average open time derived by division of total open time in a current trace in the number of closings. The current was filtered at 1 kHz and sampled at 3 kHz.

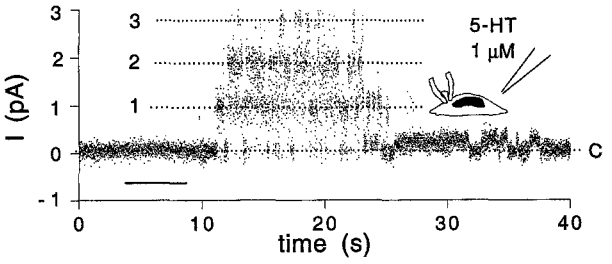

Fig. 1. Serotonin-induced single channel currents recorded in the cell-attached configuration. A typical example of 5-HT application (1 μM, horizontal bar) inducing openings of 1, 2 or 3 channels simultaneously (current levels indicated by dashed line). Pipette potential was +30 mV. Upward deflections indicate current flowing from the pipette into the cell. Current was filtered at 0.5 kHz and sampled at 20 Hz. Solutions in the bath and the pipette contained (in mM): KCl 20, NaCl 120, $CaCl_2$ 2.

further. The peak activity of the channels in four cells appeared 23 ± 4 sec after the onset of serotonin application. The duration of the averaged current, triggered by several serotonin applications (decay to 1/2 maximum in 8.8 ± 1.4 sec, $n = 4$, *not shown*) was similar to the durations of both the whole-cell serotonin-induced potassium current and the increase in $[Ca^{2+}]_i$, which we had recorded previously in C6 cells [21]. The average patch current during the response to 5-HT is about 1 pA (Fig. 1). If the area of the whole-cell membrane was about 500-fold larger than that of the cell-attached patch, then the expected whole-cell response would be about 500 pA, indeed comparable to our previous results [21]. In contrast, the large variability from patch to patch of the spontaneous channel activity precludes such comparison with the resting membrane of the whole cell. Moreover, the spontaneous channel activity was so unstable during prolonged cell-attached recordings—either gradually decreasing, or gradually increasing–that some of the repetitive 5-HT application could not induce discernible responses.

In the cell-attached configuration, the selectivity of the channels could be examined by varying $[K^+]$ in the bath and/or in the pipette ($[K^+]_o$, $[K^+]_p$, respectively) and applying ramp voltage pulses to the patch membrane (Fig. 2*A*). In this configuration, the reversal potential (V_{rev}) of the single channel currents depended on the ratio between $[K^+]_o$ and $[K^+]_p$, only slightly deviating from the combined Nernst equations for K^+ for the patch and the cell membranes in series (*see* Fig. 2*B*, dashed line and Eq. (1) in the legend). This indicates that potassium was the main permeating ion in the channel, as well as in the whole cell membrane, accompanied by minor permeabilities to other ions. The unitary conductance of both the spontaneous and 5-HT-evoked single channels in symmetrical $[K^+]$ (in the pipette and

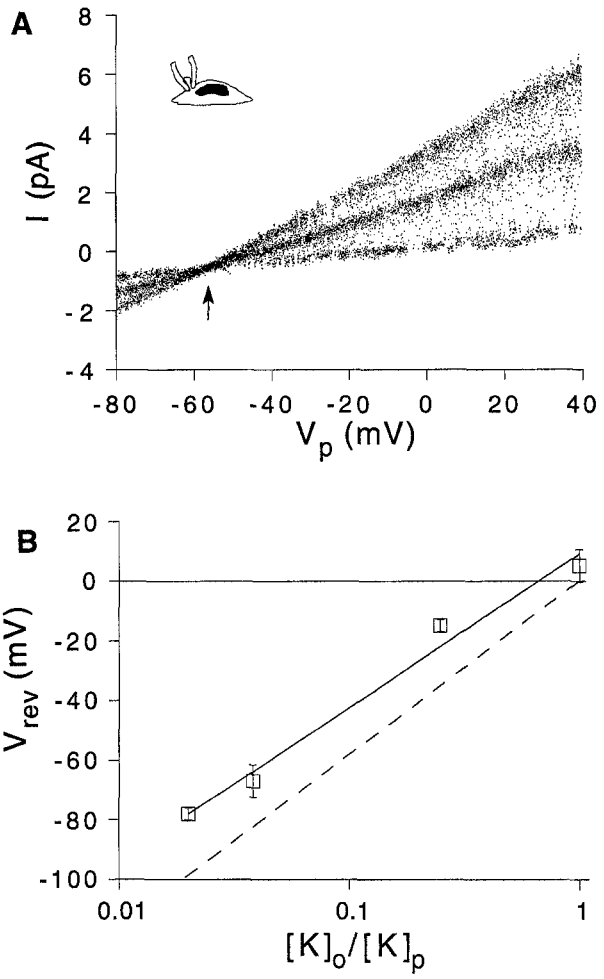

Fig. 2. The selectivity for K^+ of single channels in cell-attached configuration. (*A*) Spontaneous current fluctuations during a ramp voltage command from −80 to 40 mV (V_p) lasting 1.8 sec (time scale translated to a voltage scale on the abscissa). Upward deflections indicate current flowing from the pipette into the cell through two flickery channels. The reversal potential (V_{rev}, arrow, of zero current at pipette potential relative to ground) was −55 mV and the single channel conductance was 25 pS. Solutions (in mM) bath: KCl 5, NaCl 135, $CaCl_2$ 2; pipette: KCl 140, Na 0, Ca 0. (*B*) Symbols: V_{rev} (mean ± SEM of 3–5 cells) with various combinations of Na^+ and K^+ activities (Cl^- salt, *see* Materials and Methods) in the recording pipette ($[K^+]_p$) and in the extracellular solution ($[K^+]_o$). Dashed line: calculated V_{rev}, based on the assumption that both the true reversal potential of the channel, E_{rev}, and the cell resting potential, E_M (both defined as the potential difference between the cytoplasm and the external ground), equal the appropriate Nernst potentials for K^+:

$$\begin{aligned} V_{rev} &= E_M - E_{rev} \\ &= -(RT/F)\ln([K^+]_i/[K^+]_o) + (RT/F)\ln([K^+]_i/[K^+]_p) \\ &= (RT/F)\ln([K^+]_o/[K^+]_p), \end{aligned} \quad (1)$$

where $[K^+]_i$ is the intracellular potassium activity and R, T and F are, respectively, the universal gas constant, temperature (°K) and Faraday constant.

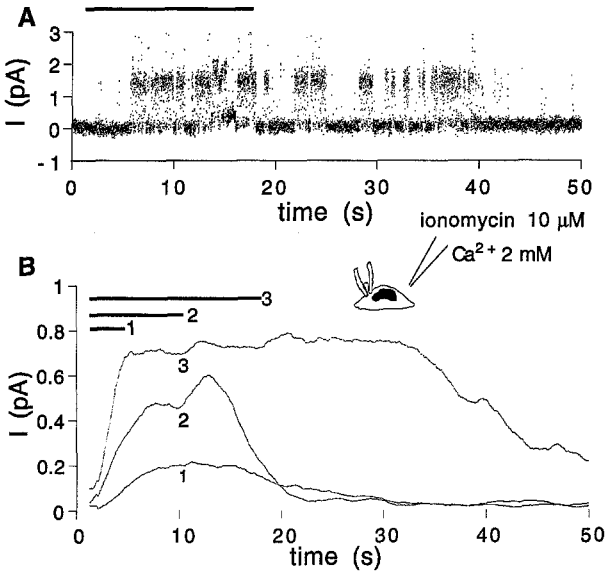

Fig. 3. Ionomycin-induced single channel currents in cell-attached configuration. Positive current flows from the pipette into the cell. Both the bath and the pipette solutions were Ca^{2+} free. (*A*) Applications (bars) of ionomycin (10 μM) and calcium (2 mM) induced channel openings. The current was filtered at 0.5 kHz and sampled at 200 Hz. (*B*): Superimposed averages (1, 2 and 3) of 13–25 successive responses to repeated applications of ionomycin (horizontal bars, numbered respectively). Longer ionomycin applications induced larger and more prolonged responses. Current responses were filtered at 0.5 kHz and sampled at 40 Hz. The averaged current was smoothed by a 50-point running average. Solutions (in mM) bath: KCl 2.8, NaCl 140, Ca^{2+} 0; pipette: KCl 140, NaCl 0, Ca^{2+} 0. Pipette potential was 0 mV.

in the cell), measured by ramp voltage commands, was roughly 23 pS (Table 1) and their mean open time was roughly 4.5 msec. From the similarity of the open time and the conductance, we concluded that the spontaneous and the serotonin-activated channels were identical.

Potassium conductance induced by 5-HT in C6 cells is mediated by a rise in $[Ca^{2+}]_i$. We therefore investigated the direct activation of the channels by $[Ca^{2+}]_i$. No channel openings were observed in cell-attached configuration when both the bath and the pipette solutions were calcium free. This suggests that the spontaneous occurrence of channels depended, albeit indirectly, on external Ca^{2+}. In these conditions, repeated applications of both calcium (2 mM) and the calcium ionophore ionomycin (5 μM) resulted in repeated activation of channels (Fig. 3*A*) comparable to those induced by 5-HT (Table 1). The averaged single channel response was proportional to the duration of pressure ejections of ionomycin (Fig. 3*B*). Based on these findings, we conclude that in the cell-attached recordings the ionomycin-induced channels were identical to the spontaneously active and the 5-HT-induced channels.

The selectivity for K^+, the conductance and the Ca^{2+} dependence place all these three manifestations of the channel in the category of the SK channels.

Direct Channel Activation by $[Ca^{2+}]_i$

To quantify the $[Ca^{2+}]_i$ dependence of this SK channel, we used excised membrane patches in the I-O configuration. No channel openings were observed in calcium-free bath solution or in 50 nM $[Ca^{2+}]_i$ (Ca^{2+} buffered with 1 mM BAPTA). Multiple openings of fast-gated channels were observed at $[Ca^{2+}]_i$ ranging from 150 nM up to 2.5 mM, the highest concentration investigated (Figs. 4 and 5). At this configuration, the channel activity was dependent, reversibly and reproducibly, on $[Ca^{2+}]_i$ at the exposed intracellular face of the patch (Fig. 4*A*). The unitary conductance, measured by ramp voltage commands (*not shown*) was 26 ± 12 pS in symmetric 140 mM KCl, similar to that of the serotonin and ionomycin-activated channels in the cell-attached configuration (Table 1). The unitary current jump of 1.16 ± 0.01 pA at a holding potential of −50 mV (cytoplasmic side negative) did not vary significantly at the different $[Ca^{2+}]_i$. In addition, at supramicromolar $[Ca^{2+}]_i$, we observed larger and prolonged current jumps (Fig. 4, at 250 μM). The two types of opening modes will be denoted sf (small-fast) and LS (large-slow) levels.

We were unable to obtain patches with only one channel (except for one case). Furthermore, the total number of channels in a patch was uncertain, and their gating characteristics varied at different $[Ca^{2+}]_i$ levels (Fig. 4). Therefore, initially, rather than calculating the opening probability, we used the mean current (I_{mean}) across the patch as an indicator of channel activity. I_{mean} increased in a biphasic manner as a function of $[Ca^{2+}]_i$ (Fig. 5, circles). The first activation phase extended over a submicromolar $[Ca^{2+}]_i$ range (half plateau level of 0.4 pA at 400 nM $[Ca^{2+}]_i$, Hill coefficient 3, *see* Fig. 5 legend).

To estimate the average number, $\bar{n}$, of open levels of a particular type at different $[Ca^{2+}]_i$, we analyzed 10 patches in the following way: First, by "eyeballing" the current records, we determined the correspondence between the open levels in the record and the particular peaks in their amplitude histogram. This was facilitated by the differences between amplitudes of the channel in the two modes of opening (*see, for example,* Fig. 4, *A* and *B*). Secondly, after separating the peaks into two types, we calculated $\bar{n}$, the average number of open channels of a given type, using the following equation:

$$\bar{n}_x = \frac{\sum_{i=0}^{n_x} W_{i_x} i_x}{\sum_{i=0}^{n_x} W_{i_x}}, \qquad (2)$$

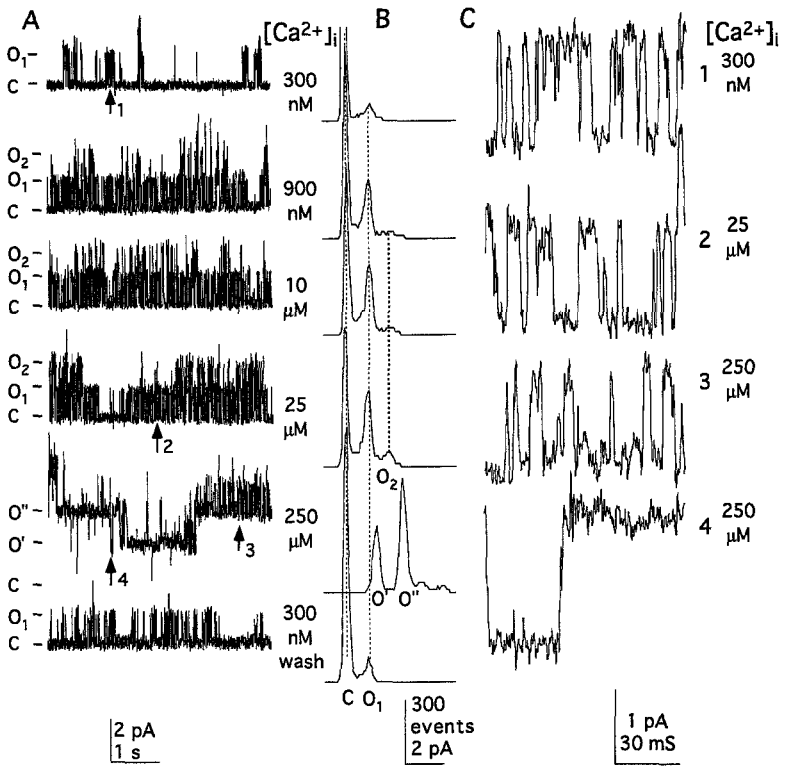

Fig. 4. $[Ca^{2+}]_i$-induced channel opening in the I-O configuration. Single channel currents from a single patch, with the indicated $[Ca^{2+}]_i$ on the exposed cytoplasmic side of the patch. The membrane potential was −50 mV (cytoplasmic side negative, openings and inward current indicated by upward deflections), in symmetrical 140 mM KCl. (*A*) Current traces illustrate channel activity (between closed, *C* and several open, *O* levels). Note the increase in activity when $[Ca^{2+}]_i$ is raised above 300 nM (top to bottom), and the return to low opening rate upon wash with $[Ca^{2+}]_i$ of 300 nM. Note also that, while between 900 nM and 25 μM the activity of at least three channels appears to have reached stability, $[Ca^{2+}]_i$ of 250 μM induced prolonged openings to two levels (indicated by *O′*, *O″*), superimposed with fast gating activity and seldom closings to the basal (*C*) level. (*B*) The matching amplitude histograms of the current traces. Vertical dashed lines indicate the closed (*C*), and open fast-gated levels. (O_1 and O_2). Note the larger (1.2–1.3 fold) amplitudes (*O′* and *O″*) of the slow-gated current steps at 250 μM $[Ca^{2+}]_i$. (*C*) Segments of the current traces in *A* (indicated by arrows) on an expanded time scale. Note the fast-gated openings found at all $[Ca^{2+}]_i$ vs. the slow-gated openings at $[Ca^{2+}]_i$ of 250 μM. Current was filtered at 500 Hz and sampled at 1 kHz. Submicromolar $[Ca^{2+}]_i$ was buffered with 1 mM BAPTA, supramicromolar $[Ca^{2+}]_i$ was not buffered.

where the subscript x refers to level type—sf or LS; i_x is the opening level number of type x; W_{i_x} is the weight of the peak in the histogram, corresponding to this opening level; and n_x is the total number of peaks of a particular level type in the histogram.

If we assume sf and LS to be two modes of opening of one SK channel, rather than two independent types of channels, the probability of the opening (P_o) of the channel can be approximated. At the range of submicromolar $[Ca^{2+}]_i$, which induced openings mainly of sf levels, P_o of the SK channel was estimated by dividing $\bar{n}_{sf}$ by the maximum number of channels (sf and LS combined) observed in a particular patch (Fig. 5, squares). The resulting estimate of P_o corresponding to the plateau of the dose response curve ($[Ca^{2+}]_i \approx 1$ μM) was 0.35.

Apparently, LS levels, though sporadically observed, did not contribute significantly to the mean current at submicromolar $[Ca^{2+}]_i$. At this range, I_{mean} increase was due to the increased average number of open sf levels (Fig. 6). LS levels became more prominent in the second activation phase at $[Ca^{2+}]_i \geq 100$ μM, becoming the major component at supramillimolar range (Fig. 6, dashed line). Thus, the transition between sf and LS dominance seems to occur at $[Ca^{2+}]_i$ of roughly 1–25 μM (Fig. 6).

Relationship between sf and LS states

Are sf and LS two different channels or do they represent two states of the same channel protein? We addressed this question by (i) examining the correlation between the average numbers of open sf and LS levels in the same patch, and (ii) by comparing the selectivity and conductance of both open states.

It is evident from Fig. 6 that the appearance of LS levels coincides, on average, with the sum of the average number of open levels $\bar{n}_{sf} + \bar{n}_{LS}$ exceeding unity. In patches selected according to this empirical criterion (i.e., $\Sigma\bar{n}_x > 1$), the diminishing number of sf levels was correlated with increased appearance of LS levels at a roughly 1:1 ratio (Fig. 7). This is consistent with the notion that sf and LS states constitute two manifestations of the activity of one channel.

If the LS and sf states constitute two opening modes of the same channel, and if these states are interconnected directly, such direct interconnections might be observed. Indeed, careful examination of records from two patches revealed brief transitions between openings of the sf type and openings with the same amplitude as that of the LS state but much shorter-lasting (illustrated in Fig. 8). In the same record we did not observe in-

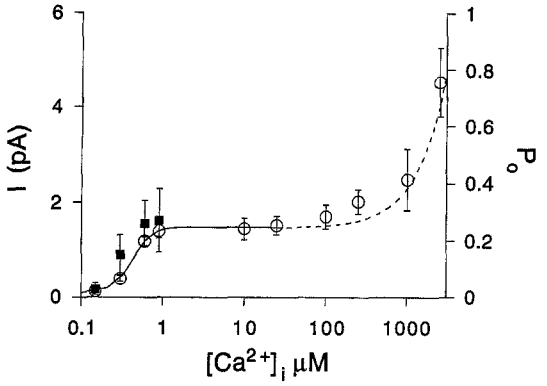

Fig. 5. Dose response of activation by $[Ca^{2+}]_i$. The average current via SK channels in an I-O configuration in the patch (○, left ordinate) as a function of $[Ca^{2+}]$ at the cytoplasmic surface. The mean current was measured by averaging the current record over 10–30 sec. Note the two phases of the activation curve. The first phase (between 150 nM and 25 μM, continuous line) was fitted with Hill equation:

$$I_{mean}([Ca^{2+}]_i) = \frac{I^{max}_{mean}}{1 + \left(\frac{K_D}{[Ca^{2+}]_i}\right)^h}, \quad (3)$$

yielding a plateau level of mean current (I^{max}_{mean}) of 1.49 ± 0.04 pA, half plateau level at $[Ca^{2+}]_i$ (K_D) of 400 ± 20 nM, and Hill coefficient (h) of 3.2 ± 0.4. The dashed line represents the second activation stage at $[Ca^{2+}]_i$ above 100 μM. P_o (■, right ordinate) at submicromolar $[Ca^{2+}]_i$ was estimated as detailed in the text. Data points represent mean ± SEM, n = 4 to 10. E_H = −50 mV (cytoplasmic side negative) in symmetrical 140 mM KCl solutions.

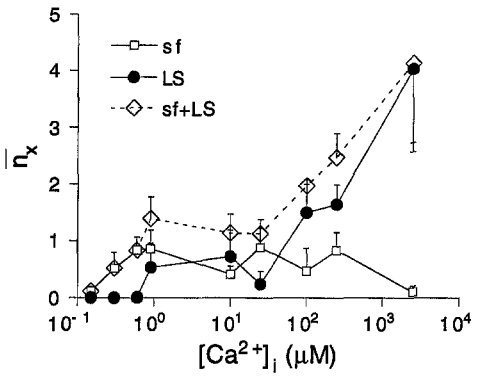

Fig. 6. $[Ca^{2+}]_i$ activation of sf and LS states. The average number of open levels ($\bar{n}_x$) of the sf (□), or LS (●) types was estimated as described in the text. Note the resemblance between the $[Ca^{2+}]_i$ dependence of the sum, $\bar{n}_{sf} = \bar{n}_{LS}$ (◇) and the $[Ca^{2+}]_i$ dependence of the average current in Fig. 5. The analysis was performed on 10 patches.

terconnections between sf and the LS state proper (i.e., long-lasting).

The SK Channel Selectivity and Conductance

In the I-O configuration, $[Ca^{2+}]_i \geq 900$ nM induced openings of both sf and LS states. E_{rev} of steady-state current fluctuations of both levels shifted from 0 mV in symmetric 140 mM KCl (Fig. 9*A*) to −30 mV when recorded with $[K^+]$ 35 mM in the pipette (adjusted by equimolar replacement of KCl with NMG/MS; Fig. 9*B*). This confirms that both modes of the channel conduct potassium and not chloride. The current-voltage relationship of the sf and LS levels was slightly nonlinear at potentials away from E_{rev}. Near E_{rev}, the respective conductances of the sf and LS states were 18 and 25 pS, respectively, in symmetric 140 mM KCl, and 6.5 and 9.6 pS, respectively, with $[K^+]_p$ of 35 mM ($[K]_o$ dependence of the conductance is discussed below). Note that, while the average current amplitudes of sf and LS do not appear to be significantly different (Fig. 9, *A* and *B*), when sf amplitude was plotted *vs.* LS amplitude, separately for each patch, the conductance ratio sf:LS was about 0.7 (0.76 with $[K^+]_p$ 140 mM and 0.67 with $[K^+]_p$ 35 mM), regardless of membrane potential (Fig. 9, *C* and *D*). The similarity of the selectivity and the constancy of the conductance ratio of the two types of open levels further support the notion that these are two states of the same channel.

The Cation Selectivity of the SK Channel

The selectivity of the channel to cations at submicromolar $[Ca^{2+}]_i$ was estimated by measuring the deviation of E_{rev} from E_K in several different solutions (Fig. 10, Table 2). In the O-O configuration, $[Ca^{2+}]_i$ was buffered to 500–600 nM with 1 mM BAPTA inducing mainly sf openings. E_{rev} was determined by ramp voltage commands. When most of external KCl was replaced by NMG/MS, the measured reversal potential closely followed E_K. E_{rev} was not affected when gluconate was substituted for Cl^- (Table 2). On the other hand, substitution of $[K^+]_o$ by either Na^+ or Ca^{2+} resulted in a deviation of the measured reversal potential from E_K. The effect was prominent in low $[K^+]_o$ range, including physiological $[K^+]_o$. The data were fitted by the Goldman-Hodgkin-Katz (GHK) equation modified to account for Ca^{2+} [32]:

$$E_{rev} = \frac{RT}{F} \ln \frac{[K^+]_o + \frac{P_{Na}}{P_K}[Na^+]_o + 4\frac{P'_{Ca}}{P_K}[Ca^{2+}]_o}{[K^+]_i + \frac{P_{Na}}{P_K}[Na^+]_i + 4\frac{P'_{Ca}}{P_K}[Ca^{2+}]_i \exp(FE_{rev}/RT)} \quad (4)$$

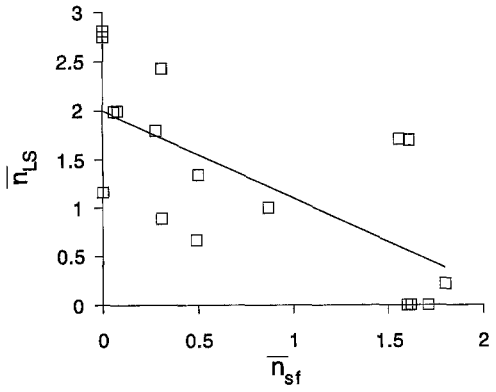

Fig. 7. The appearance of the LS states correlated with the disappearance of the sf states. The average number of open LS levels ($\bar{n}_{LS}$) plotted against the average number of open sf levels ($\bar{n}_{sf}$). Line: linear regression fit to the data (slope = −0.9, r = 0.7, P = 0.004). The analysis was performed on the 10 patches of Fig. 6, on $[Ca^{2+}]_i$ levels at which the sum $\bar{n}_{sf} + \bar{n}_{LS} > 1$.

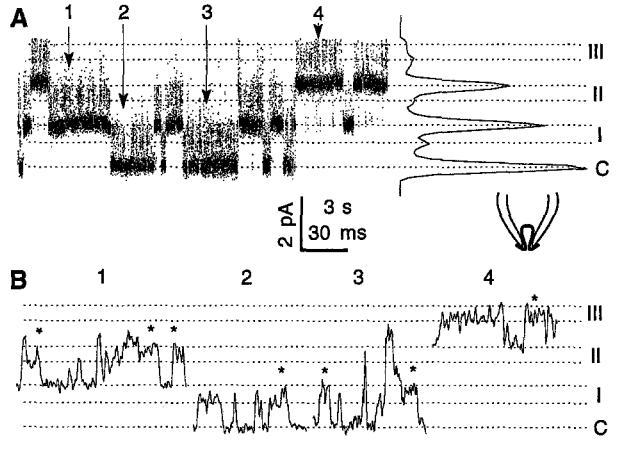

Fig. 8. Direct transitions between open sub-levels. (*A*) Current trace from an inside-out patch and the corresponding amplitude histogram in which the small peaks represent the smaller sub-levels. Horizontal dashed lines mark all levels according to histogram peaks. Upward deflections indicate current flowing into the pipette through open channels. (*B*) Segments of the trace (indicated by arrows), shown on an expanded time scale. (*) Transitions between main levels I II III and their adjacent sub-levels (0.7 pA apart); (*C*) channels closed. Symmetric 140 mM KCl solutions and 250 μM $[Ca^{2+}]_i$ at the cytoplasmic side. E_M was −50 mV (cytoplasmic side negative). Current was filtered at 1 kHz and sampled at 5 kHz.

where $P'_{Ca} = P_{Ca}/(1 + \exp(FE_{rev}/RT))$, P_{Na}, P_{Ca} and P_K are the permeabilities of Na^+, Ca^{2+} and K^+, respectively and R, F and T have their usual thermodynamic meaning. The derived permeability ratios P_K:P_{Ca}:P_{Na} were 1:0.040 ± 0.010:0.030 ± 0.008 (mean ± 95% confidence limits).

We further examined the relative Ca^{2+} permeability in the SK channel in another set of experiments us-

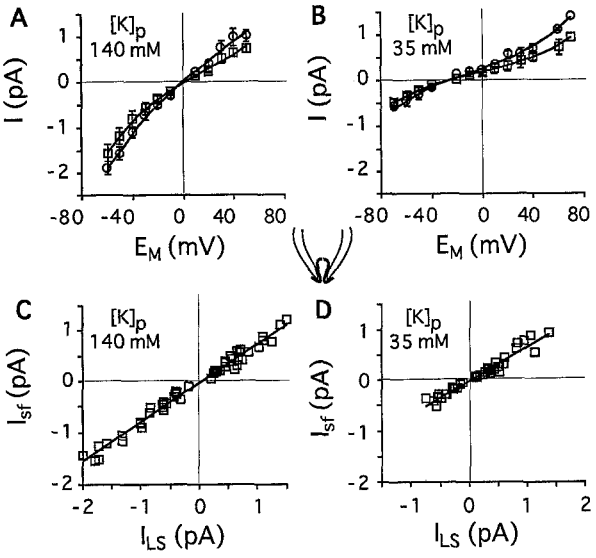

Fig. 9. Current-voltage relationships of sf and LS sub-levels. Current was recorded at the inside-out configuration. The cytoplasmic side of the patch was exposed to bath solution containing 140 mM $[K^+]_i$ and $[Ca^{2+}]_i$ ranging from 900 nM to 3 mM. The amplitudes of the current fluctuations were measured in 10 sec long records, at different holding potentials using amplitude histograms to differentiate between sf (□) and LS (○) levels. (*A*) K^+ in the pipette ($[K^+]_p$ = 140 mM. (*B*) $[K^+]_p$ = 35 mM (equimolar replacement with NMG/MS, seven patches in each group). Note E_{rev} shift from 0 to −30 mV and reduced conductance in *B* as compared to *A*. (*C* and *D*) The relationship between current amplitudes of the sf and LS levels in the same patches and $[Ca^{2+}]_i$. Lines: linear fit of data points (slopes: *C:* 0.76 ± 0.01 and *D:* 0.67 ± 0.03, r = 0.99). Note that the conductance ratio between the two levels was voltage independent.

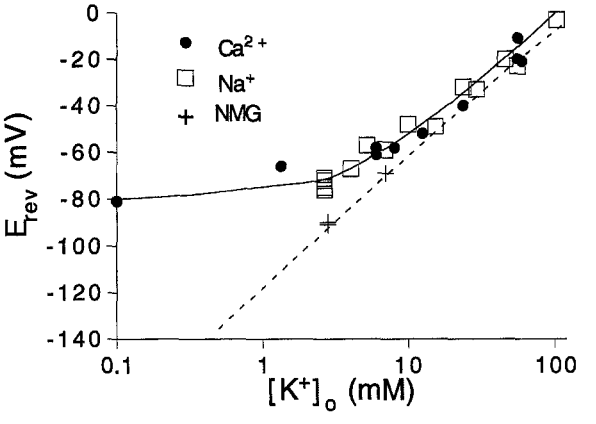

Fig. 10. The selectivity of the SK channel. E_{rev} (determined by ramp voltage commands) as a function of the ionic composition. $[K^+]_o$ (abscissa) was varied between 140 and 1.4 mM (converted to activities, *see* Table 2) by substitution with either NMG (+), Na^+ (open symbols) or Ca^{2+} (filled symbols). Dashed line: Calculated Nernst potential of K^+ (E_K). Continuous line: GHK equation modified to account for $[Ca^{2+}]$ (Eq. 4), fitted to the data points (Table 2). The best fitted values of E_{rev} were obtained with permeability ratios P_K:P_{Ca}:P_{Na} of 1: 0.040 ± 0.010: 0.030 ± 0.008 (mean ± 95% confidence limits, r = 0.97).

Table 2. Dependence of E_{rev} on the cationic composition of the external solutions (Fig. 10)

Activities (mM)[c]			E_{rev} (mV)	E_k (mV)
$[K^+]_o$	$[Na^+]_o$	$[Ca^{2+}]_o$	Measured	Calculated
0.1[a]	0	29	−81	−175
1.3[a]	0	29	−70	−111
2.7	104	1.7	−71	−92
2.7	104	1.7	−72	−92
2.7	104	1.7	−75	−92
2.7	104	1.7	−76	−92
4	104	1.7	−67	−82
5	101	1.7	−57	−76
6[a]	0	28	−58	−72
6[a]	0	28	−61	−72
7	100	1.7	−59	−68
8	99	1.7	−58	−65
10	98	1.7	−48	−59
13	0	26	−52	−54
15	96	1.6	−49	−49
24[a]	0	24	−38	−37
24	92	1.5	−32	−37
29	85	1.4	−33	−32
45	80	1.3	−20	−21
56[a]	0	16	−11	−16
56[a]	0	16	−20	−16
56	66	0.9	−23	−16
60[a]	0	16	−21	−14
104	0	0	−2	0
6[b]	0	0	−69	−68
2.7[b]	0	0	−91	−92
2.7[b]	0	0	−90	−92

E_{rev} was measured in 100 O-O patches by 2 sec ramp voltage commands. Internal solution was 140 mM KCl or potassium gluconate ([a]), 600–900 nM Ca^{2+} (buffered with 1 mM BAPTA) and 1 mM ATP. External solutions were prepared from stock solutions listed in Materials and Methods, using either Cl^- or gluconate ([a]) salts. [b]External solution containing mainly NMG/MS. [c]Activities were calculated from concentrations using activity coefficients from Table 8.9 in Robinson and Stokes [28].

ing O-O patches with KCl 140 mM and Ca^{2+} 600 nM in the pipette. E_{rev} was measured at a constant $[K^+]_o$ of 1.4 mM, while varying $[Ca^{2+}]_o$ ($CaCl_2$ substituted with NMG-Cl). $Ca^{2+}{}_o$ activities of 52, 14 and 1.7 mM were associated with mean E_{rev} of -51 ± 6 ($n = 5$), -73 ($n = 2$) and -100 ± 3 mV ($n = 4$), respectively (illustrated in Fig. 11).

Conductance Dependence on $[K^+]_o$

Partially replacing $[K^+]_o$ with other cations decreased the unitary conductance of the channel as measured by the same ramp voltage commands used to find E_{rev}. The effect was similar with either Na^+, Ca^{2+} or NMG^+ as the substitutes (*not shown*). The values of conductance *vs.* $[K^+]_o$ (obtained from equimolar substitution of K^+ with Na^+) were fitted with the Michaelis-Menten

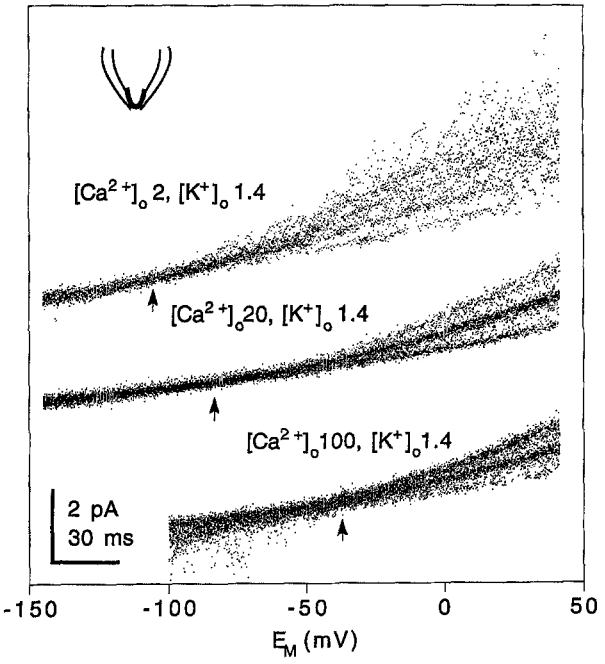

Fig. 11. The Ca^{2+} permeability of the SK channel. Determination of E_{rev} of single channel currents in O-O patches with various concentrations of $[Ca^{2+}]_o$ (in mM) and a constant $[K^+]_o$ of 1.4 mM (osmolarity adjusted to 280 mOsm with NMG). An arrow indicates the current reversal potential (E_{rev}) of superimposed 15–20 current responses to ramp voltage commands of 0.5 sec duration (converted to mV on the abscissa). E_{rev} was determined as the midpoint of the region of minimum variance of the current fluctuations, searched over a running interval of 60 data samples. Note the shift of E_{rev} with the change of $[Ca^{2+}]_o$. The pipette contained 140 mM KCl and $[Ca^{2+}]_i$ buffered to 600 nM with 1 mM BAPTA. Current was filtered at 0.5 kHz and sampled at 1 kHz.

equation yielding maximum conductance of 25 pS with half maximum at $[K^+]_o$ of 5 mM (Fig. 12).

Channel Modulation by ATP

Channel activity (at the sf level induced by $[Ca^{2+}]_i$ of 600 nM) tended to diminish spontaneously after patch excision into the O-O configuration (Fig. 13*A*). The estimated time constant of the activity decay was about 60 sec (Fig. 13*C*). This "wash-down" was prevented by the addition of 1 mM ATP to the internal solution (Fig. 13*B*). As mentioned above, we routinely included ATP in the pipette solution when studying selectivity and conductance in the O-O configuration. No such phenomenon was observed in the I-O configuration.

Discussion

In this paper we describe SK channels found in the C6 glioma cell line. We and others have already demon-

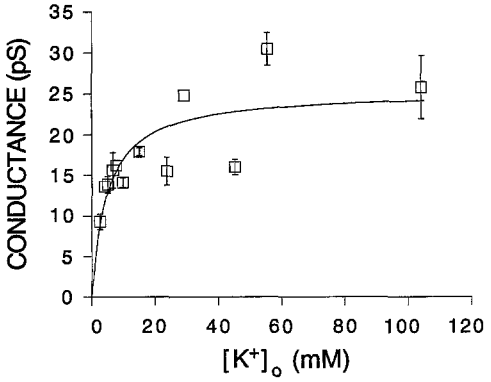

Fig. 12. $[K^+]_o$ dependence of the SK channel conductance. Conductance was measured by 2 sec ramp voltage commands in the O-O configuration. The pipette contained 140 mM KCl, $[Ca^{2+}]_i$ 500–600 nM and 1 mM ATP. $[K^+]_o$ was partially substituted with equivalent concentrations of Na^+. The conductance, measured near the reversal potential, increased as the activity of $[K^+]_o$ was raised. The data were fitted with the Michaelis-Menten equation yielding maximum conductance of 25 pS and 1/2 maximum at $[K^+]_o$ of 5 mM ($r = 0.8$).

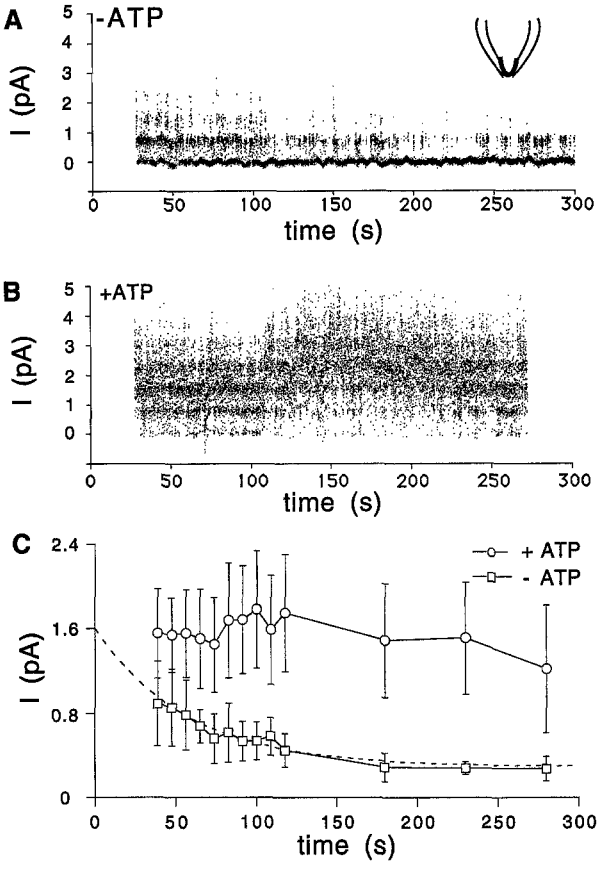

Fig. 13. ATP requirement for persistent channel activity. (*A*) In an outside-out configuration with 140 mM KCl and 600 nM Ca^{2+} in the pipette, channel activity diminished gradually. (*B*) Inclusion of 1 mM ATP in the internal solution efficiently conserved channel activity. (*C*) Current across the patch averaged over 1 sec recording periods at $E_M = 0$ mV. Each point represents mean ± SEM of six patches recorded with (○) or without (□) ATP. The time constant of activity decay without ATP, from the exponential fit to the data points, is about 60 sec (dashed line, $r = 0.98$). Time zero in *A* and *B* is the patch excision about 30 sec prior to the beginning of the recording. Note that the zero-time extrapolated value of 1.6 pA of the minus-ATP patch current is the same as would be that of the plus-ATP patch current. This value is in the range of the plateau level of I_{mean} across inside-out patches (Fig. 5).

strated that in C6 cells several transmitters, including 5-HT, can induce a $[Ca^{2+}]_i$-dependent K^+ conductance by releasing calcium from IP_3-sensitive stores [21, 23, 24, 26, 30]. The contribution of this work is a detailed characterization of the SK channel underlying this conductance change. Our major findings are: the maintenance of SK channel activity in O-O patches, as well as in whole-cell configuration [21], requires ATP; the SK channel conductance increases with $[K^+]_o$; the SK channel undergoes $[Ca^{2+}]_i$-dependent reversible transitions between two gating modes; the SK channel permeability to Ca^{2+} is not negligible.

The comparison of channels recorded in the different configurations is summarized in Table 1. Two configuration-dependent differences (not an unusual finding [13, 31]) in the channel properties are noticeable: (i) The average open time of the SK channels in the I-O configuration was considerably shorter than in other configurations; (ii) ATP maintained single channel activity in the O-O configuration (Fig. 13) and persistent whole-cell responses to 5-HT [21] but was not required in the I-O configuration. In fact, the absence of ATP in recordings from I-O patches may underlie the relative brevity of the openings in this configuration. The requirement for ATP suggests that the channel itself may be one of the ATP-supported elements in the signal transduction from 5-HT stimulation to SK-channel activation [21]. There are relatively abundant reports about phosphorylation-dependent activity of various channels, demonstrated in excised patches in the presence of "phosphorylating cocktails" including the catalytic subunits of various protein-kinases [17, 37, 38]. In contrast, there are only a few reports, where in excised patches channel phosphorylation depended on endogenous kinases [8, 35]. In some of these cases, the activity of endogenous phosphatases is implied by the phenomenon of spontaneous "rundown" of channel activity [39]. If the SK channel activity depends on phosphorylation/dephosphorylation, that no externally added kinases or phosphatases are required during the ATP-maintained channel activity indicates that these enzymatic activities may be closely associated with this channel. We are presently unaware of any comparison between inside-out and outside-out patches with respect to phosphorylation. According to the common view, the o-o patch is formed by the resealing of membrane frag-

ments, while during the excision of an i-o patch only the membrane outside the pipette rim is severed. The channel "rundown" and the requirement for ATP in the o-o configuration in our experiments suggest the activation of an endogenous phosphatase in the process of membrane reorganization.

The conductance of the single SK channel in C6 cells, determined in O-O patches from the slope of the current-voltage relationship in the vicinity of the reversal potential, was related to the extracellular concentration of the permeant K^+ ions (Fig. 12, as in other channels; [7, 18, 20]). The individual conductance values ranged from 34 pS in symmetric 140 mM KCl to 4 pS when $[K^+]_o$ was reduced to 2.8 mM. $[K^+]_o$ near active neurons is expected to fluctuate between 2.5 and 10 mM [3, 26]. Thus, the $[K^+]_o$ dependence of the conductance of the SK channels was most prominent in the physiological concentration of $[K^+]_o$ (half-maximal conductance at 5 mM $[K^+]_o$, Fig. 12). One of the roles attributed to glial cells is to buffer changes in $[K^+]_o$ to provide a microenvironment appropriate for neuronal activity [2, 12, 14, 26]. The increase of conductance following a rise in $[K^+]_o$ might enhance the effectiveness of K^+ ions removal (given a favorable electrochemical gradient to drive the ions into the glial cells).

We observed two channel types: smaller and fast-gated (sf) and larger and slow-gated (LS). The sf type was prevalent at submicromolar $[Ca^{2+}]_i$ and the LS type at supramicromolar $[Ca^{2+}]_i$ (Figs. 4 and 6). The following findings indicate that these two types of opening represent two states of the same channel: (i) both types were permeable mainly to K^+ ions (Fig. 9, *A* and *B*); (ii) the ratio between the amplitudes of the unitary current steps of the two types was very similar in different patches, independently of the holding potential (sf:LS $\approx$ 0.7, Fig. 9, C and *D*); (iii) the appearance of LS levels was correlated with the disappearance of sf levels (Fig. 7); and (iv) direct transitions between the two levels were demonstrable (Fig. 8), although, so far, only between sf levels and seemingly "destabilized" LS levels. Hence, it seems that a dynamic process of conversion between the two states occurs in a $[Ca^{2+}]_i$ range between 1 and 100 μM at the plateau of I_{mean} (Fig. 5). Interestingly, a calcium-dependent potassium channel (with larger conductance of 184 pS), with a very similar biphasic $[Ca^{2+}]_i$ activation and increasing conductance, was described in the heart sarcoplasmic reticulum [32]. There it was suggested to provide a path for counter current during the massive calcium influx to the sarcoplasm during muscle contraction. Whether this interconversion in the SK channels in C6 cells has a physiological function remains to be determined.

When considerable portions of $[K^+]_o$ were replaced by either Na^+ or Ca^{2+}, the measured reversal potential deviated from E_K (Fig. 10). The estimated K^+:Ca^{2+}:Na^+ permeability ratios were 1:0.040:0.030. The non-negligible permeability of Ca^{2+} through the SK channels was further demonstrated in another set of experiments in which external calcium was the only potentially permeant ion that was manipulated (replaced by NMG). This also resulted in depolarized E_{rev} with increasing $[Ca^{2+}]_o$ (Fig. 11). Although we could not demonstrate an actual calcium current through the channels, an intriguing possibility is that extracellular calcium may flow down its electrochemical gradient into the open SK channel further activating it. It is also possible that Ca^{2+} influx via the SK channels participates in the refilling of intracellular calcium stores (*see* [10, 34] for discussion of Ca^{2+} entering K^+ channels and [25, 33] referring to Ca^{2+}-activated cation channels).

The authors are grateful to Dr. M. Segal for continuous support, stimulating discussions and criticism throughout the course of this work, to Dr. I. Steinberg for helpful suggestions and to Dr. H. Jarosch, for helping with the Fortran application. N.M.'s research was supported in part by BARD, the U.S.-Israel Binational Agricultural Research and Development Fund, grant no. IS-1670-89RC.

References

1. Adelman, J.P., Shen, K., Kavanaugh, M.P., Warren, R.A., Wu, Y., Lagrutta, A., Bond, C.T., North, R.A. 1992. Calcium-activated potassium channels expressed from cloned complementary DNAs. *Neuron* **9:**209–216
2. Barres, B.A. 1991. New roles for glia. *J. Neurosci.* **11:**3685–3694
3. Barres, B.A., Chun, L.L.Y., Corey, D.P. 1990. Ion channels in vertebrate glia. *Annu. Rev. Neurosci.* **13:**441–471
4. Blatz, A.L., Magleby, K.L. 1986. Single apamin-blocked Ca^{2+}-activated K^+ channels of small conductance in cultured rat skeletal muscle. *Nature* **323:**718–720
5. Blatz, A.L., Magleby, K.L. 1987. Calcium-activated potassium channels. *Trends Neurosci.* **10:**463–467
6. Capoid, T., Ogden, D.C. 1989. The properties of calcium-activated potassium ion channels in guinea-pig isolated hepatocytes. *J. Physiol.* **409:**285–295
7. Christophersen, P. 1991. Ca^{2+}-activated K^+ channel from human erythrocyte membranes: Single channel rectification and selectivity. *J. Membrane Biol.* **119:**75–83
8. Chung, S., Reinhart, P.H., Martin, B.N., Brautigan, D., Levitan, I.B. 1991. Protein kinase activity closely associated with a reconstituted calcium-activated potassium channel. *Science* **253:** 560–562
9. Grandolfo, M., D'Andrea, P., Martina, M., Ruzzier, F., Vittur, F. 1992. Calcium-activated potassium channels in chondrocytes. *Biochem. Biophys. Res. Commun.* **182:**1429–1434
10. Grissmer, S., Lewis, R.S., Cahalan, M.D. 1992. Ca^{2+}-activated K^+ channels in human leukemic T cells. *J. Gen. Physiol.* **99:**63–84
11. Hamill, O.P., Marty, A., Neher, E., Sakmann, B., Sigworth, F.J. 1981. Improved patch-clamp techniques for high-resolution current recording from cell and cell-free membrane patches. *Pfluegers Arch.* **391:**85–100
12. Hill, A.V. 1910. The possible effects of the aggregation of the molecules of haemoglobin on its dissociation curves. *J. Physiol.* **40:**iv–vii
13. Horn, R., Vandenberg, C. 1986. Inactivation of single sodium channels. *In:* Ion Channels in Neutral Membranes. J.M. Ritchie,

R.D. Keynes, and L. Bolis, editors. pp. 71–83. A.R. Liss, New York
14. Inoue, I. 1981. Activation-inactivation of potassium channels and development of the potassium channel spike in internally perfused squid giant axons. *J. Gen. Physiol.* **78:**43–61
15. Jan, L.Y., Jan, Y.N. 1992. Structural elements involved in specific K^+ channel functions. *Annu. Rev. Physiol.* **54:**537–555
16. Kaczmarek, L.K., Perneu, T.M. 1991. The molecular biology of K^+ channels. *Curr. Op. Cell Biol.* **3:**663–670
17. Katsushige, O., Fozzard, H.A. 1991. Phosphorylation restores activity of L-type calcium channels after rundown in inside-out patches from rabbit cardiac cells. *J. Physiol.* **454:**673–688
18. Latorre, R., Miller, C. 1983. Conduction and selectivity in potassium channels. *J. Membrane Biol.* **71:**11–30
19. Latorre, R., Oberhouser A., Labarca, P., Alvarez, O. 1989. Varieties of calcium-activated potassium channels. *Annu. Rev. Physiol.* **51:**385–399
20. Lewis, C.A. 1979. Ion-concentration dependence of the reversal potential and the single channel conductance of ion channels at the frog neuromuscular junction. *J. Physiol.* **286:**417–445
21. Manor, D., Moran, N., Segal, M. 1992. Calcium dependence of serotonin-evoked conductance in C6 glioma cells. *Glia* **6:**118–126
22. McManus, O.B. 1991. Calcium-activated potassium channels: regulation by calcium. *J. Bioenerg. Biomembr.* **23:**537–560
23. Ogura, A., Amano, T. 1984. Serotonin-receptor coupled with membrane electrogenesis in rat glioma clone. *Brain Res.* **297:** 387–391
24. Ogura, A., Ozaki, K., Kudo, Y., Amano, T. 1986. Cytosolic calcium elevation and cGMP production induced by serotonin in clonal cells of glial origin. *J. Neurosci.* **6:**2489–2494
25. Petersen, O.H., Maruyama, Y. 1983. Cholecystokinin and acetylcholine activation of single-channel currents via second messenger in pancreatic acinar cells. *In:* Single-Channel Recording. B. Sakmann and E. Neher, editors. pp. 425. Plenum, New York
26. Reiser, G., Binmoller, F., Strong, P.N., Hamprecht, B. 1989. Activation of K^+ conductance by bradikynin and by inositol-1,4,5-trisphosphate in rat glioma cells: involvement of intracellular and extracellular Ca^{2+}. *Brain Res.* **506:**205–214
27. Renterghem, C.V., Lazdunski, M. 1992. A small-conductance charybdotoxin-sensitive, apamin-resistant Ca^{2+}-activated K^+ channel in aortic smooth muscle cells (A7r5 line and primary culture). *Pfluegers Arch.* **420:**417–423
28. Robinson, R.A., Stokes, R.H. 1965. Electrolyte Solutions. Pitman, Bath UK
29. Rudy, B. 1988. Diversity and ubiquity of K channels. *Neuroscience* **25:**729–749
30. Sugino, H., Ogura, A., Kudo, Y., Amano, T. 1984. Intracellular Ca^{2+} elevation induced by a neurotransmitter in a glial cell clone. *Brain Res.* **322:**127–130
31. Trautman, A., Siegelbaum, S.A. 1983. The influence of membrane patch isolation on single acetylcholine-channel current in rat myotube. *In:* Single-Channel Recording. B. Sakman and E. Neher, editors. pp. 473–480. Plenum, New York
32. Uehara, A., Yasukohchi, M., Ogata, S., Imanaga, I. 1991. Activation by intracellular calcium of a potassium channel in cardiac sarcoplasmic reticulum. *Pfluegers Arch.* **417:**651–653
33. von Tscharner, V., Prod'hom, B., Baggiolini, M., Reuter, H. 1986. Ion channels in human neutrophils activated by a rise in free cytosolic calcium concentration. *Nature* **324:**369–370
34. Walz, W. 1989. Role of glial cells in the regulation of the brain ion microenvironment. *Prog. Neurobiol.* **33:**309–333
35. Wang, J., Best, P.M. 1992. Inactivation of the sarcoplasmic reticulum calcium channel by protein kinase. *Nature* **359:**739–741
36. Wang, W., Sackin, H., Giebisch, G. 1992. Renal potassium channels and their regulation. *Annu. Rev. Physiol.* **54:**81–96
37. Wang, W., Giebisch, G. 1991. Dual modulation of renal ATP-sensitive K^+ channel by protein kinases A and C. *Proc. Natl. Acad. Sci. USA* **88:**9722–9725
38. White, R.E., Lee, A.B., Shcherbatko, A.D., Lincoln, T.M., Schonbrunn, A., Armstrong, D.L. 1993. Potassium channel stimulation by natiuretic peptides through cGMP-dependent dephosphorylation. *Nature* **361:**263–266
39. White, R.E., Schonbrunn, A., Armstrong, D.L. 1991. Somatostatin stimulates Ca^{2+}-activated K^+ channel through protein dephosphorylation. *Nature* **351:**570–573